

# Measurement of Cosmogenic $^{32}\text{P}$ and $^{33}\text{P}$ Activities in Rainwater and Seawater

Claudia R. Benitez-Nelson\* and Ken O. Buesseler

Woods Hole Oceanographic Institution, Woods Hole, Massachusetts 02543

**We have developed a new method for the collection, purification, and measurement of natural levels of  $^{32}\text{P}$  and  $^{33}\text{P}$  in rain, marine particulates, and dissolved constituents of seawater.  $^{32}\text{P}$  and  $^{33}\text{P}$  activities were measured using a recently developed ultra-low-level liquid scintillation counter. Measurement by liquid scintillation counting allows, for the first time, simultaneous measurement of both  $^{32}\text{P}$  and  $^{33}\text{P}$ . Furthermore,  $^{33}\text{P}$  activities are measured with high efficiency (> 50%), regardless of the amount of stable phosphorus in the sample. Liquid scintillation also produces energy specific  $\beta$  spectra which has enabled us to identify previously unrecognized  $\beta$ -emitting contaminants in natural samples. In order to remove these contaminants, new methods of purification have been developed which utilize a series of precipitations and anion and cation exchange columns. Rainwater and dissolved seawater samples were extracted from large volumes of rain- and seawater, 5–20 and >5000 L, respectively, using iron-impregnated polypropylene filters. On these filters, it was possible to load between 25 and 30%  $\text{Fe}(\text{OH})_3$  by weight, over twice that loaded on previously utilized materials. Using our collection, purification, and liquid scintillation counting techniques, it was possible to obtain specific  $^{32}\text{P}$  and  $^{33}\text{P}$  activities with less than 10% error ( $2\sigma$ ) in rainwater and 20% error ( $2\sigma$ ) in seawater.**

A new technique has been developed for the extraction, purification, and measurement of  $^{32}\text{P}$  (half-life, 14.28 days) and  $^{33}\text{P}$  (half-life, 25.3 days) in rain, marine particulates, including plankton, and dissolved inorganic and organic phosphorus. These two cosmogenic radioisotopes are removed from the atmosphere predominantly via wet precipitation.<sup>1–3</sup> Due to their short half-lives and reactivity toward atmospheric aerosols,  $^{32}\text{P}$  and  $^{33}\text{P}$  have shown great utility in the determination of stratospheric/tropospheric air mass exchange and tropospheric air mass and aerosol residence times.<sup>1,2,4–6</sup>

More recently,  $^{32}\text{P}$  and  $^{33}\text{P}$  have been used in an attempt to elucidate the short term biogeochemical cycling of P within the upper ocean by measuring the activities of these isotopes in

various dissolved and particulate biological pools.<sup>7–12</sup> Phosphorus is an essential nutrient, and one of the main obstacles in furthering our understanding of upper ocean biogeochemical cycling is the lack of reliable nutrient uptake and export rate data. Thus, any direct measurements of nutrient turnover within the marine biological cycle are of great importance. However, both atmospheric and marine investigations that utilize  $^{32}\text{P}$  and  $^{33}\text{P}$  have been hampered by the extremely low levels found in natural environments. Average concentrations of  $^{32}\text{P}$  and  $^{33}\text{P}$  in rainwater range from 0.2 to 6 dpm/L, whereas in seawater, dissolved  $^{32}\text{P}$  and  $^{33}\text{P}$  concentrations are 1000 times lower.<sup>7–12</sup> Hence, preconcentration from several thousand liters of seawater and ultra-low-level counting techniques are needed.

$^{32}\text{P}$  and  $^{33}\text{P}$  both decay via  $\beta$  emission with maximum energies ( $E_{\text{max}}$ ) occurring at 1.71 and 0.249 MeV, respectively. Until now,  $^{32}\text{P}$  and  $^{33}\text{P}$  activities have been determined by counting a hygroscopic precipitate,  $\text{NH}_4\text{MgPO}_4 \cdot 6\text{H}_2\text{O}$ , on an anticoincidence low-level  $\beta$  counter.<sup>4,7–13</sup> The combined  $^{32}\text{P}$  and  $^{33}\text{P}$  activities have been separated by taking advantage of the differences in the relative  $E_{\text{max}}$  intensity of the two isotopes.<sup>7,11,14</sup> Briefly, because  $^{33}\text{P}$  is a low-energy  $\beta$  emitter, its  $\beta$  emission is easily blocked by increasing sample thickness and/or by the presence of an external absorber. In contrast,  $^{32}\text{P}$ , due to its relatively high  $E_{\text{max}}$  is only minimally affected by absorption. Thus, for measurement of both isotopes, P samples are counted twice: once with an external absorber to block  $^{33}\text{P}$  activity and only measure  $^{32}\text{P}$ , and again without the absorber to measure the total activity. The  $^{33}\text{P}$  activity is then found by the difference between the two count rates.

The efficiency of  $\beta$  detection for  $^{32}\text{P}$  is often between 25 and 50% using anticoincidence low-level  $\beta$  counting.<sup>2</sup> The efficiency of  $^{33}\text{P}$ , on the other hand, is highly dependent on the thickness of the  $\text{NH}_4\text{MgPO}_4 \cdot 6\text{H}_2\text{O}$  precipitate to be counted and is much less than 20%. Thus, measurement of  $^{33}\text{P}$  requires low levels of stable P (i.e., less precipitate) within the sample. This makes  $^{33}\text{P}$  measurement in eutrophic environments very difficult. In addition, changes in sample geometry caused by the nature of the

- (1) Lal, D.; Peters, B. In *Handbuch der Physik* 46/2; Flugge, S., Ed.; Springer Verlag: New York, 1967; pp 551–612.
- (2) Waser, N. A. D. Ph.D. Thesis, MIT/WHOI, 1993.
- (3) Waser, N. A. D.; Bacon M. P. *Geophys. Res. Lett.* **1994**, *21*, 991–994.
- (4) Goel, P. S.; Rama Thor; Zutshi, P. K. *Tellus* **1959**, *9*, 91–100.
- (5) Bhandari, N.; Lal, D.; Rama Thor J. *Geophys. Res.* **1970**, *75*, 2974–2980.
- (6) Walton, A.; Fried, R. E. *J. Geophys. Res.* **1962**, *67*, 5335–5340.

- (7) Lal, D.; Lee, T. *Nature* **1988**, *333*, 752–754.
- (8) Lal, D.; Chung, Y.; T. Platt, T.; Lee, T. *Limnol. Oceanogr.* **1988**, *33* (6, part 2), 1559–1567.
- (9) Lee, T.; Barg, E.; Lal, D. *Limnol. Oceanogr.* **1991**, *36*, 1044–1053.
- (10) Lee, T.; Barg, E.; Lal, D. *Anal. Chim. Acta* **1992**, *260*, 113–121.
- (11) Waser, N. A. D.; Fleer, A. P.; Hammer, T. R.; Buesseler, K. O.; Bacon, M. P. *Nucl. Instrum. Methods in Phys. Res.* **1994**, *A388*, 560–567.
- (12) Waser, N. A. D.; Bacon, M. P.; Michaels, A. P. *Deep-Sea Res.* **1996**, *43*, 421–436.
- (13) Lal, D.; Rama Thor; Zutshi, P. K. *J. Geophys. Res.* **1960**, *65*, 669–673.
- (14) Lal, D.; Schink, D. *Rev. Sci. Instrum.* **1960**, *31*, 395–398.

hygroscopic precipitate will alter the  $^{33}\text{P}$  detection efficiency. Also, the low-level  $\beta$  counters provide only gross counts. Thus, any interference due to other short-lived  $\beta$  emitters present in the sample are not easily distinguished from the relatively small sample signal. Samples must be counted repeatedly to allow for time and half-life comparisons between sample and expected values in order to verify that the sample is free of other  $\beta$  emitters. This only works if the half-lives of the two isotopes of interest are considerably different and the activities are large. Depending on the efficiency and background of the low-level  $\beta$  detectors, and assuming high purity and reasonably low counting errors, between 1 and 2 L ( $^{33}\text{P}$  activity  $\geq 0.3$  dpm) of rainwater and  $\geq 1000$  L of low-stable P seawater ( $\leq 0.3$  mM) are needed for measurement of both  $^{33}\text{P}$  and  $^{32}\text{P}$ .

An alternative approach is to use low-level background liquid scintillation spectrometry (LSS). LSS produces energy-specific  $\beta$  spectra, and recent developments in LSS technology have reduced background levels to less than 3 cpm over the entire energy spectrum. Background can be further reduced to less than 1.5 cpm by defining specific  $^{33}\text{P}$  and  $^{32}\text{P}$  regions of interest. As a result, it is now possible to measure low levels of  $^{33}\text{P}$  and  $^{32}\text{P}$  activity ( $^{33}\text{P}$  activity  $\geq 0.5$  dpm) with LSS. The advantages of using LSS over low-level  $\beta$  counters are numerous. Both  $^{32}\text{P}$  and  $^{33}\text{P}$  can be counted simultaneously and with significantly higher efficiencies ( $>50\%$  for both  $^{32}\text{P}$  and  $^{33}\text{P}$ ). In addition, samples with low amounts of stable P are not required in order to achieve such high efficiencies. Evidence of contamination by other  $\beta$  emitters can be determined by analyzing spectra for evidence of anomalous peaks that are not readily apparent when traditional  $\beta$  counters are used.

In the following, a new technique is described for the collection, purification, and separate determination of  $^{33}\text{P}$  and  $^{32}\text{P}$  in rain- and seawater using LSS. In each section, we describe a detailed procedure and discuss how each differs from previous work. Results from rain- and seawater measurements are shown thereafter.

#### SAMPLE COLLECTION

The measurement of  $^{32}\text{P}$  and  $^{33}\text{P}$  in rainwater and in seawater requires the extraction of these isotopes from relatively large amounts water. In this study, we have utilized the strong affinity of phosphorus in all forms onto iron-impregnated filters in order to achieve this goal. However, numerous tests had to be conducted in order to first ensure good extraction efficiency of P over the course of sample collection. In rain water, there is typically little to no stable phosphorus.<sup>15</sup> In contrast, in seawater, dissolved P is divided into two main pools: dissolved inorganic (DIP) and dissolved organic (DOP) phosphorus. Both are comprised of a wide range of chemical compounds, which have yet to be fully quantified and most likely have large variations in chemical reactivity. Traditional measurements of P in the ocean sciences, as well as in this study, define DIP as that fraction which reacts to form a molybdenum blue complex in the presence of ascorbic acid.<sup>16</sup> DOP is calculated as the difference between total

dissolved phosphorus (TDP) and DIP. TDP is measured here using the acid persulfate method.<sup>16</sup>

**Iron Filter Preparation.** Previous researchers utilized the impregnation of acrilan fibers with  $\text{Fe}(\text{OH})_3$ .<sup>8-10</sup> However, in this study, 25  $\mu\text{m}$  pore size polypropylene sheets (MWM Co., 1 Newbury St., Quincy, MA 02171) are impregnated with iron instead of acrilan fibers. Filters were first impregnated with 6.25 N NaOH at 85–90 °C for 10–15 min, allowed to cool, and rinsed with distilled water. The filters were then impregnated with a 50%  $\text{FeCl}_3$  solution at 85–90 °C for 15 min, allowed to cool, and placed in a 3 N  $\text{NH}_4\text{OH}$  bath for several hours.<sup>17</sup> Filters were subsequently rinsed and stored in a plastic bag. Certified ACS  $\text{FeCl}_3$  used in the impregnation of the polypropylene sheets was first extracted with diisopropyl ether in order to reduce levels of stable P in the  $\text{FeCl}_3$  solution to less than 0.1  $\mu\text{mol}$  of P/g of  $\text{Fe}(\text{OH})_3$ .

Using this technique, it was possible to load between 25 and 30%  $\text{Fe}(\text{OH})_3$  by weight onto the polypropylene sheets, twice the estimated load of  $\text{Fe}(\text{OH})_3$  on acrilan fibers.<sup>8</sup> We found that the polypropylene was much easier to impregnate with Fe in a consistent and uniform manner. Furthermore, it was possible to obtain much better water flow through the polypropylene sheets.

**Extraction Experiments.** We checked the extraction efficiency of DIP from freshwater and both DIP and DOP from seawater on these new adsorbers. As expected, extraction efficiency increased with increased loading of  $\text{Fe}(\text{OH})_3$  and care was taken to ensure a relatively consistent maximum loading of between 25 and 30%  $\text{Fe}(\text{OH})_3$  by weight on the polypropylene filters. Initial extraction efficiency tests were conducted with pH 7 distilled water spiked with 4.1  $\mu\text{M}$  DIP and 1.9  $\mu\text{M}$  DOP [0.5  $\mu\text{M}$  adenosine triphosphate (ATP) + 1.4  $\mu\text{M}$  glucose 1-phosphate]. The sample was then passed through a 30.5 cm long, 1.9 cm diameter (volume 0.087 L) PVC pipe packed with iron filters. Extraction was maintained at greater than 95%, with a flow rate as high as 440 mL/min over the course of 280 column volumes (25 L) of flow.

In seawater experiments, it was expected that the efficiency of extraction would be significantly altered due to differences in ion association between fresh water and salt water and the high scavenging efficiency of  $\text{Fe}(\text{OH})_3$  for a variety of other elements. In particular, it was expected that dissolved silica, which can be up to 10 times higher in concentration than TDP, would be the main chemical species to absorb and saturate the  $\text{Fe}(\text{OH})_3$  column.<sup>8</sup> Large-scale TDP extraction tests were conducted by passing 4000 L of 0.2  $\mu\text{m}$  filtered seawater (DIP 0.2–0.3  $\mu\text{M}$ ; DOP 0.45–0.5  $\mu\text{M}$ ; silicate 2–4  $\mu\text{M}$ ) through a 1.4 L volume collection tube packed with Fe-coated polypropylene at a flow rate 4–6 L/min. Extraction was maintained at greater than 95% for both DIP and DOP over the first 700 column volumes or 980 L of seawater. Extraction efficiencies decreased for both DIP and DOP to 90 and 60%, respectively, by 2850 column volumes (Figure 1a). This compares favorably with similar experiments utilizing acrilan fibers tested in this laboratory (Figure 1b) and by previous investigators.<sup>9</sup> More interestingly, the extraction efficiency differs between the DOP and DIP fractions. There is a more rapid decrease in collection efficiency for DOP relative to DIP. This is

(15) Duce, R. A. In *The Role of Air–Sea Exchange in Geochemical Cycling*; Buat-Menard, P., Ed.; D. Reidal Publishing Co. Dordrecht, The Netherlands, 1986; pp 497–529.

(16) Koroleff, F. In *Methods of Seawater Analysis*, 2nd ed.; Grasshoff, K., Ehrhard, M., Kremling, K., Eds.; Verlag Chemie: Weinheim, 1983; pp 125–135.

(17) Krishnaswami, S.; Lal, D.; Somayajulu, B. L. K.; Dixon, F. S.; Stonecipher, S. A.; Craig, H. *Earth Planet. Sci. Lett.* **1972**, *16*, 84–90.

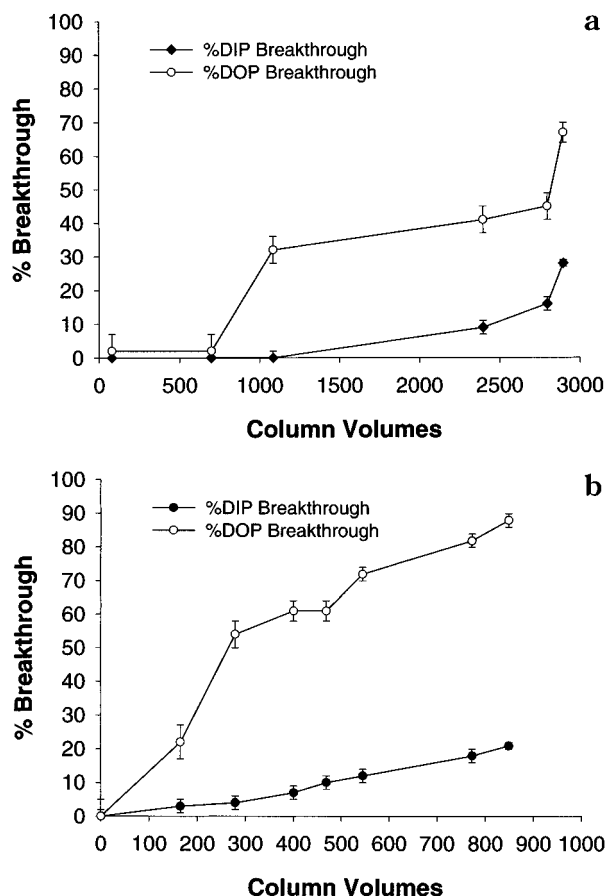


Figure 1. Collection efficiency for DIP and DOP versus column volume for a 1.4 L collection tube. Percent breakthrough is defined by the measured DIP and DOP concentrations in the pipe effluent relative to that entering. Errors are  $2\sigma$  as determined by replicate analysis. (a) Iron-coated polypropylene; (b) iron-coated acrilan.

true for acrilan fibers as well (Figure 1b). This is not surprising given the wide range in reactivity expected from the known chemical species of DOP.<sup>19</sup> The observed difference in absorption between DIP and DOP necessitates that little or no P should be allowed to pass through (breakthrough) the iron absorbers during sample collection. Otherwise, fractionation of the two reservoirs would result in  $^{32}\text{P}$  and  $^{33}\text{P}$  measurements that would be difficult to interpret within the context of biological cycling in the system. Therefore, the size of the iron extraction cartridge utilized in extracting dissolved  $^{32}\text{P}$  and  $^{33}\text{P}$  must be varied in accordance with the seawater volume to be sampled in order to maintain 95% TDP extraction efficiency.

**Field Sampling: Rainwater.** Rainwater was collected from the roof of Clark Laboratory, at the Woods Hole Oceanographic Institution (WHOI) in Woods Hole, MA (41°32.11'N, 70°38.89'W). The extraction of  $^{32}\text{P}$  and  $^{33}\text{P}$  from rainwater was modified so that  $^7\text{Be}$  and  $^{210}\text{Pb}$  activities could be measured separately via  $\gamma$  counting. Rain samples were spiked with 100  $\mu\text{mol}$  of stable P (as  $\text{Na}_3\text{PO}_4 \cdot 12\text{H}_2\text{O}$ ), Pb (as  $\text{PbNO}_3$ ), and Be [as  $\text{Be}_4\text{O}(\text{C}_2\text{H}_3\text{O}_2)_6$ ] as yield monitors and passed through a 30.5 cm long, 1.9 cm diameter (volume 0.087 L) PVC pipe packed with iron filters. It

was found that by adjusting the pH of the rain sample to less than 1.5, TDP was still collected with an efficiency greater than 70%, while less than 10% of the  $^7\text{Be}$  and 50% of the  $^{210}\text{Pb}$ , were absorbed. This allowed for two separate samples: one containing  $^{32}\text{P}$  and  $^{33}\text{P}$ , the other,  $^7\text{Be}$  and  $^{210}\text{Pb}$ . The filtrate was then prepared for  $^7\text{Be}$  and  $^{210}\text{Pb}$  measurement via  $\gamma$  detection.<sup>18</sup>

**Field Sampling: Seawater.** Seawater samples were collected in Wilkinson Basin in the Gulf of Maine. Between 4000 and 6000 L of seawater were passed sequentially through two parallel 10 and 1  $\mu\text{m}$  polypropylene Hytrec prefilters, and two 0.2  $\mu\text{m}$  pleated polypropylene membrane cartridges (25.4 cm long, 7.6 cm diameter) before passing through three parallel 61 cm long, 7.6 cm diameter PVC pipes (volume 2.7 L) packed with  $\text{Fe}(\text{OH})_3$ -impregnated polypropylene filters. Sample volumes were maximized in order to obtain the largest possible dissolved  $^{32}\text{P}$  and  $^{33}\text{P}$  activities. PVC pipe sizes were chosen in order to maintain DIP and DOP extraction efficiencies at greater than 95% based on our earlier smaller scale experiments. Prefilters were selected to obtain different size classes of suspended particulate matter. A 1 in. inside diameter pool hose was attached to the ship's weighted hydrowire, placed over the side, and lowered to variable depths between the sea surface and 110 m. Water was then pumped using a 0.75 horsepower bronze gear pump (Teel, 1B416). Flowmeters were placed at the end of each pipe to monitor variations in flow due to packing; flow rates averaged between 3 and 4 L/min through each pipe. Pressure gauges were also placed between the pump and 10  $\mu\text{m}$  prefilter and between the 0.2  $\mu\text{m}$  prefilter and  $\text{Fe}(\text{OH})_3$  cartridges. The pressure varied from 15–20 psi at the first gauge to 40–45 psi at the second. The 20 psi increase in pressure was due to the  $\text{Fe}(\text{OH})_3$  columns rather than the 0.2  $\mu\text{m}$  prefilter. In order to check for TDP breakthrough, additional samples were taken from the filtrate and analyzed for both DIP and DOP (see Results).

## SAMPLE PROCESSING

The chemical purification techniques utilized here are similar to those employed in earlier studies and involve a series of P-specific precipitations and ion-exchange chromatography<sup>10–12</sup> (Figure 2). Modifications have been made, however, to effect complete removal of  $\beta$ -emitting contaminants such as  $^{210}\text{Pb}$  and its radioactive daughter  $^{210}\text{Bi}$ . On the basis of these modifications, we conclude that both potential contaminants were not efficiently removed by previous purification methods<sup>4,8,10–13</sup> (see following).

**Ashing and Dissolution.** The 10, 1, and 0.2  $\mu\text{m}$  Hytrec prefilters and the  $\text{Fe}(\text{OH})_3$  filters utilized for both rain- and seawater were ashed in a muffle furnace at 500 °C for 4 hours to reduce the volume of the sample and to convert all of the phosphorus to inorganic forms. It was found that the polypropylene material combusted much more cleanly to  $\text{CO}_2$  at high temperatures than the previously used acrilan fibers. The 10 and 1  $\mu\text{m}$  prefilters were then extracted with a mixed solution of 8 N  $\text{HNO}_3$  and 30%  $\text{H}_2\text{O}_2$  on low heat for at least 12 h, while the 0.2  $\mu\text{m}$  and  $\text{Fe}(\text{OH})_3$  filters were extracted with a mixed solution of 8 N  $\text{HCl}$ , and 30%  $\text{H}_2\text{O}_2$ .  $\text{HNO}_3$  was used when possible in order to achieve more rapid extraction of DIP and better precipitation of ammonium phosphomolybdate (see below).  $\text{HCl}$  was used to achieve optimal removal of  $\text{Fe}(\text{III})$  into diisopropyl ether. All of the samples were allowed to cool and filtered using a 934 AH

(18) Dibb, J. E. *J. Geophys. Res.* **1989**, *94*, 2261–2265.

(19) Strickland, J. D. H.; Parsons, T. R. In *A Practical Handbook of Seawater Analysis*, 2nd ed.; Fisheries Research Board of Canada, Ottawa, ON, Canada, 1972.

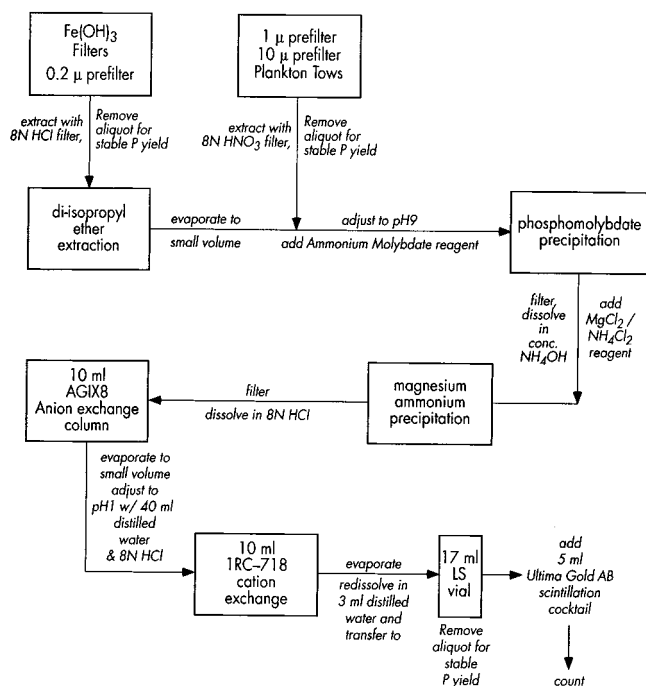


Figure 2. Chemical purification scheme.

GF/F filter, and an aliquot was removed to monitor the chemical yield of stable P during purification.

**Chemical Purification.** The 0.2  $\mu\text{m}$  prefilter and  $\text{Fe}(\text{OH})_3$  rain- and seawater samples were repeatedly extracted with diisopropyl ether until the water phase turned from brown to a pale yellow. These samples, along with the 10 and 1  $\mu\text{m}$  prefilters, were then reduced to a small volume (50 mL for the prefilters, 200 mL for the iron filters) via evaporation on a hot plate. Preliminary purification of the samples was achieved using an ammonium phosphomolybdate precipitation.<sup>21</sup> This acid-insoluble precipitate separates P from almost all other anions and cations with the exception of lead, bismuth, tin, and zirconium.<sup>20</sup>

Samples were heated to 45  $^{\circ}\text{C}$  and 60 mL of the ammonium molybdate reagent was added for every 0.1 g of  $\text{P}_2\text{O}_5$  present in the sample. Sample pH was adjusted prior to the addition of reagent such that the final pH of the sample with the added ammonium molybdate solution was between 0.6 and 0.8. Heating samples to temperatures greater than 50  $^{\circ}\text{C}$  caused precipitation of molybdic acid and contaminated the precipitate with metals such as Si, As, and V. Samples were stirred until the yellow ammonium molybdate precipitate appeared, at which point, samples were removed from the stir plate and allowed to settle for at least 1 h. After settling, the ammonium molybdate precipitate was vacuum filtered using a 934 AH GF/F filter and dissolved in concentrated  $\text{NH}_4\text{OH}$ . Samples were then prepared for magnesium ammonium orthophosphate hexahydrate precipitation.

The magnesium ammonium precipitation, while not a purification step, is necessary in order to dissolve the sample in an acidic

medium for ion-exchange chromatography. After dissolution of the first precipitate in  $\text{NH}_4\text{OH}$ , the samples were cooled in an ice bath and the pH lowered to 3–4 with 8 N HCl. Approximately 10 mL of the  $\text{MgCl}_2/\text{NH}_4\text{Cl}_2$  reagent<sup>21</sup> was added for every 0.1 g of  $\text{P}_2\text{O}_5$  in the sample solution. Concentrated  $\text{NH}_4\text{OH}$  was then added slowly to the sample, with stirring, until a white precipitate formed. Excess  $\text{NH}_4\text{OH}$  was added, and the precipitate allowed to settle for at least 1 h. The magnesium ammonium orthophosphate hexahydrate was vacuum filtered through a 934 AH GF/F filter and dissolved in 8 N HCl with low heat.

Further purification of the samples is accomplished using ion-exchange chromatography. The sample solution in 8 N HCl was first passed through a 10 mL anion-exchange column packed with  $\text{AG1} \times 8$  100–200 mesh resin (Bio-Rad) in order to remove any residual Fe(III) in the sample and other elements such as Cu, Cd, and Zn. This step was necessary as it was found that, in the subsequent cation-exchange separation steps, phosphate would be retained from dilute acid media as a result of coabsorption when Fe(III) was present. The sample was then evaporated to a small volume ( $\leq 1$  mL) and the pH adjusted to between 0.8 and 1 with slightly basic distilled water (total volume 40 mL). The solution was then passed through a 10 mL column packed with a weakly acidic cation-exchange resin, Amberlite IRC-718 (iminodiacetate group, Rohm and Haas Co.) to remove any residual  $^{210}\text{Pb}$  and  $^{210}\text{Bi}$  in the sample.

Once the sample had been purified using the IRC cation-exchange resin, solutions were carefully evaporated to dryness, taking care not to overheat the sample. After evaporation, the sample was dissolved in 1 mL of distilled water and transferred via a glass pipet to a preweighed 17 mL nonstatic liquid scintillation (LS) vial (available from Packard Industries). The beaker was then carefully rinsed twice with exactly 1 mL portions of distilled water and transferred to the LS vial. The vial was weighed, a 50  $\mu\text{L}$  aliquot removed to track chemical recovery, and 5 mL of Ultima Gold AB (Packard) scintillation cocktail added. The Ultima Gold AB cocktail is an organic solvent containing a blend of alkyl-naphthalene and PPO and bis-MSB scintillators. This cocktail was chosen because it is biodegradable, is able to incorporate higher acidity samples at relatively high sample-to-cocktail ratios, and has low associated background. No other cocktails were tested.

**Contaminant Identification.** Evidence of  $^{210}\text{Pb}$  and  $^{210}\text{Bi}$  contamination was first apparent in initial rain measurements when the Amberlite IRC column was not utilized. Samples were counted repeatedly on the LSS. Measured half-lives and region of interest backgrounds were compared with the expected backgrounds and known half-lives of  $^{32}\text{P}$  and  $^{33}\text{P}$  using a nonweighted linear least-squares curve fitting routine. Sample counts were first curve fitted using the known half-lives of  $^{32}\text{P}$  and  $^{33}\text{P}$  and the backgrounds calculated. It was found that the calculated sample background counts were significantly higher than those determined from chemistry blanks (i.e., distilled water samples processed identically to the rain samples) for both the  $^{32}\text{P}$  and  $^{33}\text{P}$  regions. Furthermore, there was significant disagreement between the measured  $^{32}\text{P}$  and  $^{33}\text{P}$  signals and their known half-lives when the background was fixed at the expected chemical blank background of 1.0 cpm and the  $^{32}\text{P}$  and  $^{33}\text{P}$  half-lives allowed to vary (Figure 3). Upon

(20) Karl-Kroupa, E.; Van Wazer, J. R.; Russell, C. H. In *Scott's Standard Methods of Chemical Analysis*; Furman, N. H. Ed.; D. Van Nostrand Co., Inc.: Princeton, NJ, 1961; Vol. 1, pp 809–813.

(21) Whaley, T. P.; Ferrara, L. W. In *Environmental Phosphorus Handbook*; Griffith, E. J., Beeton, A., Spencer, J. M., Mitchell, D. T., Eds.; Wiley: New York, 1973.

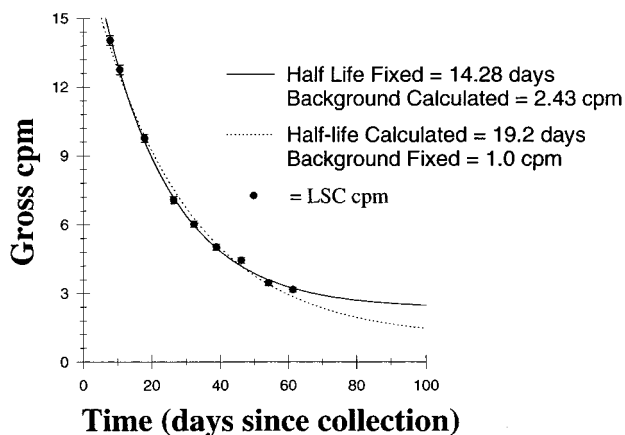


Figure 3. Decay curve analysis for  $^{32}\text{P}$  in a rain sample collected April 2, 1996 at WHOI; evidence of sample contamination. Circles are gross  $^{32}\text{P}$  cpm data points, the solid line is with the half-life fixed and a calculated background, the dotted line is with the background fixed and the half-life calculated.

closer analysis of the LSS  $\beta$  spectra, it became apparent that, during decay of  $^{32}\text{P}$  and  $^{33}\text{P}$ , a small peak emerged beneath the two. All of these factors pointed to a significant contaminant in the sample. Analysis of radioactive nuclides commonly found in rain, coupled with LSS spectral analysis, indicated that the  $\beta$  decay of both  $^{210}\text{Pb}$  and  $^{210}\text{Bi}$  was contaminating the sample. Due to the chemical manipulation of the samples,  $^{210}\text{Pb}$  and  $^{210}\text{Bi}$  were being removed to different, unknown extents. In effect, once "purified",  $^{210}\text{Bi}$  was either growing in or decaying into secular equilibrium with its parent  $^{210}\text{Pb}$ .

After testing a number of ion-exchange resins at various pH and carrier media, the IRC-718 cation-exchange resin proved to be the most efficient in fully removing any residual  $^{210}\text{Pb}$  and  $^{210}\text{Bi}$  from the sample without loss of P. Previous investigations used 10 mL columns packed with a strongly acidic cation-exchange resin Dowex 50 (sulfonic acid group, Bio-Rad Industries), in acidic media ranging from 0.1 to 9 N HCl. At both 0.1 and 9 N, tests conducted in this laboratory indicated that a small fraction of the  $^{210}\text{Pb}$  and  $^{210}\text{Bi}$  was still present in the sample (0.1–0.5% of initial or 1–3 dpm each).

It is not clear what effect  $^{210}\text{Pb}$  and  $^{210}\text{Bi}$  has had on earlier investigations using previously published ion-exchange methods and low-level  $\beta$  counting involving adsorbents to separate  $^{32}\text{P}$  and  $^{33}\text{P}$ . Our experience in rain collected at the Woods Hole Oceanographic Institution is that the  $^{210}\text{Pb}$  and  $^{210}\text{Bi}$  contaminants would cause an underestimation of 10% of the  $^{32}\text{P}$  activity ( $^{210}\text{Bi}$  ingrowth) and a 10% overestimate in the  $^{33}\text{P}$  activities (higher background due to  $^{210}\text{Pb}$ ) when samples were counted repeatedly with time and curve fitted (see below). Those studies which counted  $^{32}\text{P}$  and  $^{33}\text{P}$  samples only once and maintained fixed detector backgrounds would be expected to have even larger contributions from  $^{210}\text{Pb}$  and  $^{210}\text{Bi}$  contamination in the  $^{32}\text{P}$  and  $^{33}\text{P}$  signal. It should be noted that, in samples counted with the LSS, it was possible to remove the contaminants  $^{210}\text{Pb}$  and  $^{210}\text{Bi}$  by restricting the regions of interest, although this restriction resulted in loss of counting efficiency.

**Chemical Purification Yields and Blanks:** Yields of chemical purification ranged from 50 to 100% but were typically greater

than 80%. Most of the phosphorus lost in the chemical purification procedure occurred during the diisopropyl ether extractions, where some phosphate partitioned into the ether phase with the iron. Further P loss occurred due to absorption onto the walls of the glass beaker if samples were allowed to go dry and bake during the evaporation steps. Iron-impregnated filters were chemically processed and counted on the liquid scintillation counter to determine both stable and  $^{32}\text{P}$  and  $^{33}\text{P}$  backgrounds. Radioactive phosphorus activities were below detection and background counts were, within counting statistics, the same as the Ultima Gold AB scintillation cocktail.

Stable P blanks, while less than  $1\ \mu\text{M}$  for the chemicals used in purification, were significant, although reproducible [ $7.51 \pm 1.18\ \mu\text{mol}$  of P/g of  $\text{Fe}(\text{OH})_3$ ], for the iron-impregnated polypropylene filters. This P blank was equivalent to <10% of the total stable P spike added to rain but close to 25% of the total measured natural stable P levels in high TDP ( $\sim 1.25\ \mu\text{M}$ ) seawater samples. This would pose a problem for tracking total yields of samples retrieved from oligotrophic marine environments, as the blank stable P could be considerably greater than the actual P in the sample. Most of the stable P contamination appeared to come from the polypropylene filters. Repeated extraction of the polypropylene filters with hot 8 N HCl did not reduce stable P levels to any extent. However, extraction with 6.25 N NaOH at high temperatures and the utilization of  $\text{FeCl}_3$  extracted with diisopropyl ether reduced the stable P on the iron-coated polypropylene filters to  $2.50 \pm 0.27\ \mu\text{mol}$  of P/g of  $\text{Fe}(\text{OH})_3$ .

#### INSTRUMENTATION

**Background.** As stated previously, liquid scintillation counting has tremendous advantages over conventional  $\beta$  counting because it allows for higher efficiencies in counting and the ability to count both isotopes simultaneously. All of our samples were counted using a Packard Tri-Carb 2750TR/LL LSS (Packard Instrument Co.). This particular instrument has been specifically designed for counting low level radioactive samples by utilizing both burst counting circuitry (BCC) and a newly developed high-density, high- $\gamma$  cross-section detector guard consisting of bismuth germanate,  $\text{Bi}_4\text{Ge}_3\text{O}_{12}$  (BGO), to reduce background.<sup>22</sup> In liquid scintillation counting, background consists of both quenchable (32%) and unquenchable (68%) events. Quenchable background is caused by the interaction of high-energy cosmic rays interacting directly with the scintillation cocktail to produce photons similar to those produced by radioactive sample decay. Unquenchable background events, principally Cerenkov events, are caused by cosmic ray interactions with the vial wall and photomultiplier tubes.

Cosmic rays interact with the BGO guard to produce scintillations which primarily consist of a single burst followed by a number of afterpulses which can last up to  $5\ \mu\text{s}$ . In general, a larger number of afterpulses will occur after an unquenchable event than after a true scintillation event, especially for low-energy  $\beta$  events. The Packard TR2750/LL reduces background via burst counting circuitry which discriminates against unquenchable background by rejecting those events with afterpulses that exceed a user-determined, delay before burst (DBB), preset threshold.

(22) Passo, C. J.; G. T., *Cook Handbook of environmental liquid scintillation spectrometry. A compilation of theory and methods*; Packard Instruments: Meriden, CT, 1992; pp 1-1–1-15.

This threshold has a preset range between 75 and 800 ns. Thus, afterpulses resulting from the interaction of cosmic rays with the BGO guard can be eliminated by adjusting the DBB. Furthermore, the BGO guard passively reduces background by preventing some cosmic rays from reaching the sample.

**Instrument Optimization.** Optimization of the LSS was conducted using known amounts of  $^{32}\text{P}$  and  $^{33}\text{P}$  tracer. Both radioisotopes are commercially available from New England Nuclear Life Sciences Products and are certified to within 1% at the millicurie level ( $2.22 \times 10^6$  dpm). However, because our laboratory was interested in measuring much lower activities, a more precise measurement of  $^{32}\text{P}$  and  $^{33}\text{P}$  activity was necessary. Briefly, known aliquots of  $^{32}\text{P}$  and  $^{33}\text{P}$  ranging between 30 to 100 dpm were evaporated on stainless steel planchettes and counted on  $2\pi$  Riso anticoincidence low-level  $\beta$  detectors.<sup>11</sup> Measurement of  $^{32}\text{P}$  was conducted with an external Al foil ( $18 \text{ mg/cm}^2$ ), in order to block  $\beta$  emission from any longer lived  $^{33}\text{P}$  impurities contained within the  $^{32}\text{P}$  solution. Efficiencies of  $^{32}\text{P}$  and  $^{33}\text{P}$  were then determined by using calibrated  $\beta$ -emitting analogs,  $^{147}\text{Pm}$  ( $E_{\text{max}} = 0.224$ ) for  $^{33}\text{P}$  and  $^{234}\text{Pa}$  ( $E_{\text{max}} = 1.13$ ) for  $^{32}\text{P}$  counted under similar geometries. Efficiencies were  $28.5 \pm 0.3$  and  $55 \pm 0.4\%$  respectively, very similar to those found previously.<sup>11</sup>

Once the  $^{32}\text{P}$  and  $^{33}\text{P}$  activities were determined, it was possible to maximize the LSS settings for simultaneous measurement of  $^{32}\text{P}$  and  $^{33}\text{P}$ . High-activity, 30–50 dpm, samples were counted on the LSS in low-level count mode with the static controller on, over a range of DBB settings. The goal was to maintain the lowest possible background (B) while still maintaining high efficiency (E), such that the figure of merit ( $E^2/B$ ) was maximized for both the low-energy  $\beta$  emitter  $^{33}\text{P}$  and the high-energy  $\beta$  emitter  $^{32}\text{P}$ .<sup>22</sup> Based on this parameter, a DBB of 450 ns was chosen.

**Quench Correction.** During evaporation and transfer of the sample to a LS vial, it was found that small amounts of residual acid caused variable levels of quench. Sample size did not appear to be as significant. Simply put, quench is a measure of the photon production within the sample system, such that the higher quench, the fewer photons are produced, and hence the lower the counting efficiency. Quench further causes the  $^{32}\text{P}$  and  $^{33}\text{P}$  LS peaks to shift to lower energies within the chosen energy regions of interest. In the Tri-Carb 2750/LL, the degree to which sample quenching occurs is parameterized by the tSIE value, or the transformed spectral index of an external standard,  $^{133}\text{Ba}$ . This parameter is a function of the end point of the external standard and varies from 1000, no sample quenching, to 0, for a fully quenched sample. Because of the variances in quench and its effect on efficiency, it is critical to generate quench curves, i.e., standards of similar activity, but quenched to different degrees. We utilized both 8 N  $\text{HNO}_3$  and 8 N  $\text{HCl}$  as quenching agents in all of our quench curves. Separate curves were made with Ultima Gold AB Cocktail spiked with either  $^{32}\text{P}$  or  $^{33}\text{P}$ . Because our samples tended to be of very low activity, an additional “blank” quench correction curve, Ultima Gold AB with quenching agent only, was necessary. As expected, efficiencies changed relative to the given quench level and chosen region of interest (Figure 4). It should be noted that changing the regions will further influence the efficiency curve. Thus, care must be taken to choose regions appropriate for differing sample quenches. In rainwater samples, tSIE values ranged from 100 to 480, while in seawater

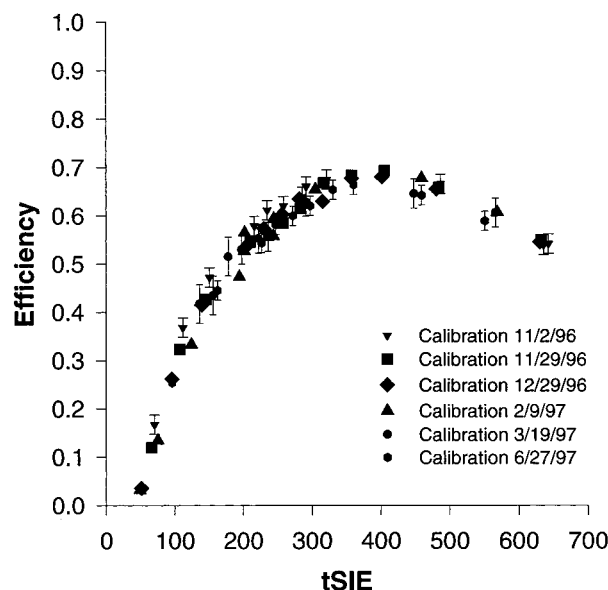


Figure 4. Quench curves for  $^{33}\text{P}$  in the 10–90 keV region, over the last 6 months. Error bars are determined from counting statistics. The shape of the  $^{32}\text{P}$  quench curves are identical to those shown for  $^{33}\text{P}$ .

samples, tSIE values ranged from 90 to 350, primarily due to variations in acidity and, in the case of seawater, substantially higher concentrations of trace constituents, such as Fe(II). Quench values between repeat counts normally did not vary by more than 10 tSIE units. If larger variations in tSIE occurred, individual counts were converted to activities prior to decay curve analysis.  $^{32}\text{P}$  and  $^{33}\text{P}$  efficiencies ranged between 50 and 70% and rarely varied by more than 2.5% ( $2\sigma$ ) between counts. Regions of interest were selected to maintain both  $^{32}\text{P}$  and  $^{33}\text{P}$  efficiencies greater than 50% in all samples.

The  $^{32}\text{P}$  and  $^{33}\text{P}$  quench correction curves further allowed for determination of the amount of  $^{32}\text{P}$  in the  $^{33}\text{P}$  region of interest. Because of the asymmetrical nature of LSS peaks, the amount of activity of  $^{32}\text{P}$  falling in the  $^{33}\text{P}$  region (10–90 keV), needed to be determined (Figure 5). In most of our samples, the contribution of  $^{32}\text{P}$  in the  $^{33}\text{P}$  window normally did not exceed 10% of the corrected  $^{33}\text{P}$  activity. This correction was determined by analyzing the distribution of  $^{32}\text{P}$  and  $^{33}\text{P}$  counts within each region of interest over the range of sample quench values.

**Instrument Stability.** Quench curves and Ultima Gold AB blanks were run repeatedly over the course of 1 year. Efficiencies for both  $^{32}\text{P}$  and  $^{33}\text{P}$  changed by less than 5% with tSIE (Figure 4). Small variations were probably more likely due to the use of different stock solutions, which were each calibrated separately, and to slight variances in pipetting and LSS vials, rather than to the actual instrument variability. Instrument blanks varied between regions of interest but remained very stable within a given region. For example, over the course of 6 months, 5 mL of Ultima Gold AB scintillation cocktail (tSIE  $\sim 645$ ) was counted for 300 min once a week. Blank cpm in the 10–90 keV window averaged  $0.95 \pm 0.05$  cpm, while blank cpm in the 90–1700 keV window averaged  $0.89 \pm 0.09$  cpm.

**Counting Procedure and Limit of Detection.** Rain- and seawater samples were counted with the low-level mode and static controller on, and a DBB of 450 ns. Samples were dark adapted

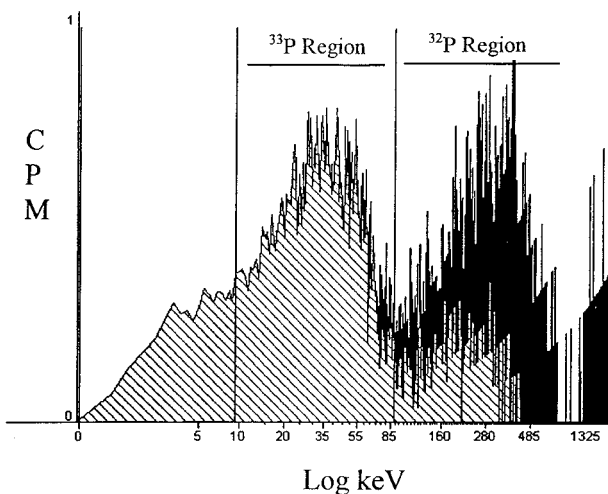


Figure 5. Liquid scintillation spectra of a rain sample collected on 6/17/97 at WHOI. Spectra is shown in cpm versus log keV in order to better show the separation of the two P isotopes.

for 6 h, allowed to cool to ambient LSS temperature, and counted repeatedly (5–10 times) over the course of 1–2 months for a period of 300 min. In this manner, it was possible to compare known and measured half-lives. Count times were shorter than optimal due to the large number of samples that needed to be counted over the relatively short decay period of time. As a result, the minimum detectable count rate at the 95% confidence limit,  $L_d$ , was limited to 0.3 cpm for both  $^{32}\text{P}$  and  $^{33}\text{P}$  in our samples.<sup>23</sup> In this scenario,  $L_d$  is defined by the following:

$$L_d = (2.71 + 4.65 \mu_s^{0.5}) / T$$

where  $T$  is the total count time in minutes and  $\mu_s$  is the mean number of total background counts registered within the region of interest during the same counting period. For our samples, increasing counting times to 1440 min (24 h) reduces the limit of detection by 50% but does not allow for adequate half-life resolution. Assuming total purity of  $^{32}\text{P}$  and  $^{33}\text{P}$ , the ultimate detection limit of  $^{32}\text{P}$  and  $^{33}\text{P}$  by ultra-low-level liquid scintillation counting is 0.1 and 0.18 cpm, or twice the standard deviation of the background cpm within the  $^{33}\text{P}$  and  $^{32}\text{P}$  regions of interest (10–90, 90–1700 keV), respectively.

#### DATA ANALYSIS, SOURCES OF ERROR, AND REPRODUCIBILITY

Each sample was counted 5–10 times, and the counts were corrected for  $^{32}\text{P}/^{33}\text{P}$  overlap. The activity of  $^{32}\text{P}$  and  $^{33}\text{P}$  at sample collection was then determined using the characteristic half-life of each isotope and a weighted nonlinear least-squares curve-fitting routine. Calculated backgrounds were then compared with that of the known scintillation cocktail blank at a given quench. Use of the curve-fitting procedure significantly improved precision and reduced the uncertainty associated with the sample and detector background. Furthermore, it enabled us to determine whether there were any other  $\beta$ -emitting isotopes in the sample that would interfere with the background and/or the half-life fit.

(23) Currie, L. A. *Anal. Chem.* **1968**, *40*, 586–593.

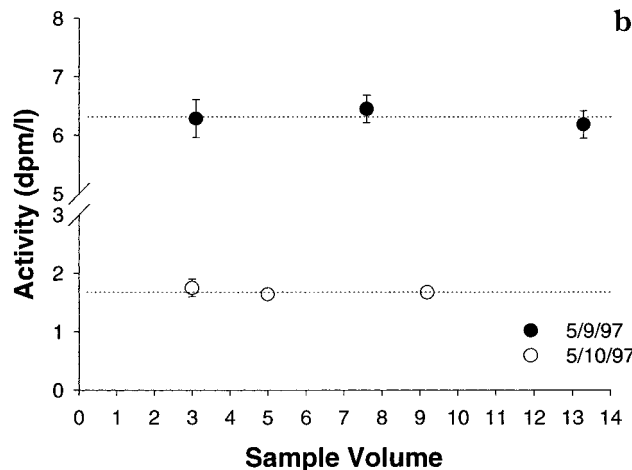
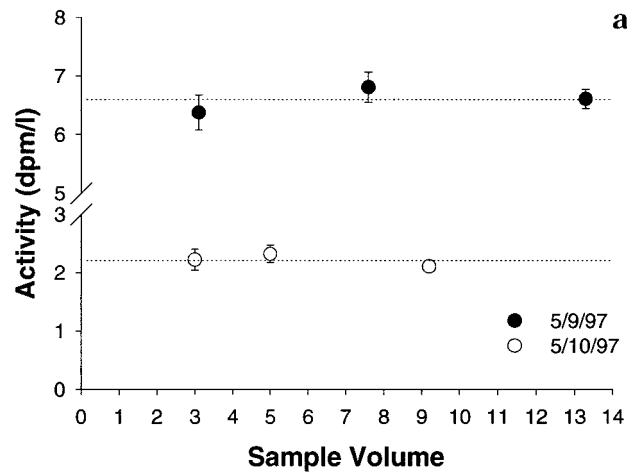


Figure 6. Activity of  $^{32}\text{P}$  and  $^{33}\text{P}$  for two rain samples collected 5/9/97 and 5/10/97 (open circles) and split into three unequal portions (sample volume). Dashed lines represent average values. (a)  $^{32}\text{P}$  (dpm/L); (b)  $^{33}\text{P}$  (dpm/L).

Table 1.  $^{32}\text{P}$  and  $^{33}\text{P}$  Activities in Individual Rain Events Collected during June and July 1996 at the Woods Hole Oceanographic Institution (41°32.11'N, 70°38.89'W)<sup>a</sup>

sample	tSIE	chemical yield (%)	$^{33}\text{P}$ (dpm/L)	$\pm$ error	$^{32}\text{P}$ (dpm/L)	$\pm$ error	$^{33}\text{P}/^{32}\text{P}$	$\pm$ error
6/17/96	312	78.5	3.27	0.17	3.86	0.12	0.84	0.05
6/20/96	305	84.0	1.12	0.11	1.63	0.08	0.69	0.08
6/22/96	320	85.7	3.87	0.10	4.10	0.18	0.94	0.05
7/1/96	275	43.8	2.42	0.12	3.09	0.10	0.78	0.05
7/12/96	477	31.6	0.54	0.05	0.61	0.06	0.88	0.12
7/15/96	452	66.0	0.58	0.05	0.74	0.04	0.79	0.08
7/19/96	158	90.8	1.38	0.05	2.01	0.09	0.69	0.04

<sup>a</sup> Absolute errors are  $2\sigma$ .

All of the  $^{32}\text{P}$  and  $^{33}\text{P}$  data are decay corrected to the midpoint of the collection period. The error on each  $^{32}\text{P}$  and  $^{33}\text{P}$  activity measurement is produced from the propagation of uncertainties from the nonlinear least-squares curve fit, detector calibration, and chemical recoveries. Overall errors for  $^{32}\text{P}$  and  $^{33}\text{P}$  activities measured in rain samples are between 3 and 10%. Larger errors are associated with those rain samples having low chemical recoveries (<10%), incomplete removal of  $^{210}\text{Pb}$  and  $^{210}\text{Bi}$  (earliest

Table 2.  $^{32}\text{P}$  and  $^{33}\text{P}$  Activities in Selected Samples Collected during March and April 1997 from Wilkinson Basin, the Gulf of Maine ( $42^{\circ}29.41'\text{N}$ ,  $69^{\circ}45.02'\text{W}$ )<sup>a</sup>

sample	volume (L)	chemical yield (%)	$^{33}\text{P}$ (dpm/m <sup>3</sup> )	$\pm$ error	$^{32}\text{P}$ (dpm/m <sup>3</sup> )	$\pm$ error	$^{33}\text{P}/^{32}\text{P}$	$\pm$ error
March, 5 m, TDP	4334	90.2	4.56	0.79	5.60	0.97	0.82	0.20
April, 5 m, TDP	6492	82.1	3.11	0.47	3.61	0.57	0.86	0.19
March, 5 m, suspended matter (10–102 $\mu\text{m}$ )	4334	99.0	0.51	0.13	0.70	0.18	0.73	0.26
		dpm/mg of P		dpm/mg of P				
April, 0–110 m, integrated plankton tow (>335 $\mu\text{m}$ )		86.8	0.28	0.02	0.23	0.01	1.23	0.12

<sup>a</sup> Absolute errors are  $2\sigma$ .

collected rain samples), or low number of repeat counts (<3). Seawater samples, generally had larger errors between 8 and 25%, predominantly due to the extremely low natural  $^{32}\text{P}$  and  $^{33}\text{P}$  activities (0.89–32.08 cpm) and our inability to count samples for a longer length of time.

In order to confirm the reproducibility of our  $^{32}\text{P}$  and  $^{33}\text{P}$  activity measurements, two rain samples, one with high total P activity (collected 5/9/97), the other with relatively low total P activity (collected 5/10/97), were spiked with stable phosphorus and split into three unequal fractions. Each fraction was then passed through a set of iron filters, purified, and counted on the LSS. tSIE values in the three 5/9/97 rain fractions varied (200–280), such that the chosen  $^{32}\text{P}$  and  $^{33}\text{P}$  regions, efficiency, and background were different between each fraction. Results of both rain samples are shown in Figure 6. There is no difference in the calculated  $^{32}\text{P}$  or  $^{33}\text{P}$  activity regardless of volume, chemical blank, or efficiency correction.

## RESULTS

**Rain.** Results of several rain samples collected during single rain events in June and July of 1996 from the roof of Clark Laboratory at the Woods Hole Oceanographic Institution are shown in Table 1. These rain samples were chosen to help illustrate the variation in chemical yield and the tSIE values encountered. In our rain samples, chemical recoveries were typically greater than 80%, with tSIE values averaging  $310 \pm 75$ . Specific activities of  $^{32}\text{P}$  and  $^{33}\text{P}$  ranged from 0.5 to 4.1 dpm/L, in single rain events, slightly higher than the average range of activities measured previously.<sup>1,2,4–6</sup> This is most likely due to both the higher  $^{33}\text{P}$  efficiency achieved in LSS and the identification and removal of contaminants. The average ratio of  $^{33}\text{P}/^{32}\text{P}$  was fairly constant over the 1 month period, averaging  $0.80 \pm 0.09$ , quite similar to the  $0.82 \pm 0.13$  measured previously in a combined 2 week sample by anticoincidence low-level  $\beta$  counting at WHOI in April of 1991.<sup>2</sup> Our rain data again indicate the higher precision and accuracy capable with LSS.

**Marine Samples.** Results are also given for some measurements of marine particulates and dissolved phases of seawater, collected in Wilkinson Basin in the Gulf of Maine during two cruises conducted in March and April of 1997 (Table 2). Chemical recoveries were typically greater than 80%. These samples represent the first  $^{32}\text{P}$  and  $^{33}\text{P}$  activities to be measured in a coastal, high-P environment. The marine particulate and dissolved samples resulted from filtration of 4300–6500 L of seawater. In

these surface TDP samples, no breakthrough of P occurred. However, in one of the deep TDP samples (not shown here), breakthrough did occur in one of the three, 2 L extraction tubes, most likely due to higher deep silicate concentrations. Regardless, breakthrough of DIP (<20% of the total), and DOP (<35% of the total) in the tube, occurred toward the end of the filtration period, such that less than 20% of the total sample volume was affected. Slightly larger collection tubes will alleviate this small problem in the future. Dissolved surface activities of  $^{32}\text{P}$  and  $^{33}\text{P}$  ranged from 1.5 to 5.6 dpm/m<sup>3</sup>. These activities are similar in magnitude, but higher than the surface  $^{32}\text{P}$  activities of 0.2–2.0 dpm/m<sup>3</sup> found off the coast of California.<sup>7,8,10</sup> This is easily explained by the higher input fluxes of  $^{32}\text{P}$  and  $^{33}\text{P}$  activity found in rainwater at the Gulf of Maine site and the ability to measure  $^{33}\text{P}$  with better efficiency. The measured ratio of  $^{33}\text{P}/^{32}\text{P}$  found in the dissolved constituent of seawater and in the >10  $\mu\text{m}$  particulate fraction are similar to that found in rain, indicating rapid turnover of P on the order of a few days. The activities of  $^{32}\text{P}$  and  $^{33}\text{P}$  and the ratio of  $^{33}\text{P}/^{32}\text{P}$  found in the >335  $\mu\text{m}$  plankton sample are also within the range of activities found previously.<sup>7,8,11,12</sup>

The ratio of  $^{33}\text{P}/^{32}\text{P}$  found in the >335  $\mu\text{m}$  plankton sample was significantly higher,  $1.23 \pm 0.12$ , than that found in the dissolved and particulate seawater fractions. This difference in activity ratio provides a powerful tool for determining the relative in situ turnover times of P between plankton and dissolved seawater. Using a simple continuous uptake model, described in detail by a previous researcher,<sup>2</sup> the average residence time of P in the >335  $\mu\text{m}$  plankton is 46 days. In contrast, if plankton ingest P early during their lifetime, and then stop feeding, the residence time of P, described by a simple age decay equation,<sup>2</sup> is 17 days. More intensive models, which include the speciation or life cycles of the collected plankton, and the cycling of P within the smaller size fractions, i.e., bacterial pools, will substantially increase our knowledge of P cycling in coastal marine environments.

## CONCLUSIONS

A new technique for the collection, purification, and measurement of  $^{32}\text{P}$  and  $^{33}\text{P}$  in rain and in various phases of marine systems is described. For the first time, it is now possible to measure  $^{33}\text{P}$  and  $^{32}\text{P}$  in single rain events and in coastal marine environments with high stable P concentrations. We have demonstrated that it is now possible to measure these isotopes with significantly higher accuracy than prior work. Ultra-low-level liquid scintillation

counting is a substantial improvement over low-level  $\beta$  counters, since it allows for the simultaneous measurement of  $^{32}\text{P}$  and  $^{33}\text{P}$ , and high counting efficiency of  $^{33}\text{P}$ , regardless of the amount of stable P. It has enabled us to quantify and remove previously unidentified  $\beta$ -emitting contaminants from our samples. The use of iron-coated polypropylene is also an improvement over previously used extraction methods in that it is possible to load twice the amount of  $\text{Fe}(\text{OH})_3$  on the filters. Furthermore, this material combusts cleanly to  $\text{CO}_2$  at high temperatures, reducing sample processing and increasing chemical recovery.

The ability to easily measure  $^{32}\text{P}$  and  $^{33}\text{P}$  in single rain events with high precision and accuracy will enable these isotopes to be used much more successfully in atmospheric chemistry studies, especially those characterizing tropospheric air mass and/or aerosol residence times, and the extent of stratospheric intrusion. The application of this newly developed technique in marine studies, however, is even more significant. The biogeochemical cycling of phosphorus within the euphotic zone can now be elucidated to a much higher degree with the additional measure-

ment of  $^{33}\text{P}$ , especially in coastal environments where nutrient uptake and export are greatest.

#### ACKNOWLEDGMENT

The authors thank J. E. Andrews, III, and Lary A. Ball for their help and insightful comments in the development of the phosphorus isotope method. The authors also thank Dr. D. Glover, Dr. K. C. Ruttenburg, and B. Benitez-Nelson for comments pertaining to the manuscript. This work was funded in part by the Office of Naval Research Fellowship Program, STAR Environmental Protection Agency Fellowship Program, National Science Foundation (Grant OCE-9633240), and the Woods Hole Oceanographic Institution (unrestricted funds). This is Contribution 9579 from the Woods Hole Oceanographic Institution.

Received for review July 14, 1997. Accepted October 7, 1997.<sup>⊗</sup>

AC9707500

---

<sup>⊗</sup> Abstract published in *Advance ACS Abstracts*, December 1, 1997.